

UCSF

UC San Francisco Previously Published Works

Title

Activation of liver X receptor improves viability of adipose-derived mesenchymal stem cells to attenuate myocardial ischemia injury through TLR4/NF- κ B and Keap-1/Nrf-2 signaling pathways.

Permalink

<https://escholarship.org/uc/item/2dm5d4bm>

Journal

Antioxidants & redox signaling, 21(18)

ISSN

1523-0864

Authors

Wang, Yabin
Li, Chunhong
Cheng, Kang
[et al.](#)

Publication Date

2014-12-01

DOI

10.1089/ars.2013.5683

Peer reviewed

ORIGINAL RESEARCH COMMUNICATION

Activation of Liver X Receptor Improves Viability of Adipose-Derived Mesenchymal Stem Cells to Attenuate Myocardial Ischemia Injury Through TLR4/NF- κ B and Keap-1/Nrf-2 Signaling Pathways

Yabin Wang,^{1,2,*} Chunhong Li,^{2,*} Kang Cheng,^{2,*} Ran Zhang,¹ Kazim Narsinh,³ Shuang Li,² Xiujuan Li,² Xing Qin,² Rongqing Zhang,² Congye Li,² Tao Su,² Jiangwei Chen,² and Feng Cao^{1,2}

Abstract

Aims: Clinical application of cellular therapy for cardiac regeneration is significantly hampered by the low retention of engrafted cells, mainly attributable to the poor microenvironment dominated by inflammation and oxidative stress in the host's infarcted myocardium. This study aims at investigating whether liver X receptor (LXR) agonist T0901317 will improve survival of adipose-derived mesenchymal stem cells (AD-MSCs) after transplantation into infarcted hearts. **Results:** Noninvasive *in vivo* bioluminescence imaging and histological staining showed that LXR agonist T0901317 improved the retention and survival of intramyocardially injected AD-MSCs. Moreover, combined therapy of LXR agonist and AD-MSCs inhibited host cardiomyocyte apoptosis, reduced fibrosis, and improved cardiac function, while it concomitantly decreased inflammatory cytokines (*e.g.*, tumor necrosis factor- α and interleukin-6) and increased growth factor (*e.g.*, vascular endothelial growth factor and basic fibroblast growth factor) expression in infarct myocardium. To reveal possible mechanisms, AD-MSCs were subjected to hypoxia/serum deprivation (H/SD) injury to simulate ischemic conditions *in vivo*. The LXR agonist (10^{-7} mM) improved AD-MSC survival under H/SD condition. Western blot revealed that the LXR agonist reduced TLR4, TRAF-6, and MyD88 protein expression, inhibited I κ B α phosphorylation and NF- κ B-p65 nuclear translocation, which resulted in accelerated Keap-1 protein degradation, enhanced Nrf-2 nuclear translocation, and increased HO-1 protein expression. **Innovation and Conclusion:** LXR agonist can enhance the functional survival of transplanted AD-MSCs in infarcted myocardium, at least partially, *via* modulation of the TLR4/NF- κ B and Keap-1/Nrf-2 signaling pathways. Moreover, combined therapy of LXR agonist and AD-MSCs has a synergetic effect on cardiac repair and functional improvement after infarction. *Antioxid. Redox Signal.* 21, 2543–2557.

Introduction

STEM CELL TRANSPLANTATION has emerged as a promising therapeutic strategy for ischemic heart disease (11, 13, 28). Among all cell candidates for cardiac regeneration, adipose-derived mesenchymal stem cells (AD-MSCs) are considered an optimal cell type for clinical application, as they can be easily obtained from adipose tissue (26). How-

ever, low retention and poor survival of injected stem cells are major obstacles to achieve intended therapeutic effect. Our previous studies revealed that nearly 90% of the stem cells might not survive within the first 4 days after cell delivery because of ischemia and local inflammation (6, 41). Other studies demonstrated that improving the conditions of this unfavorable niche in infarcted myocardium could increase the survival of injected stem cells (31, 39). Our group

¹Department of Cardiology, PLA General Hospital, Beijing, China.

²Department of Cardiology, Xijing Hospital, Fourth Military Medical University, Xi'an, Shaanxi, China.

³Department of Radiology, UC San Diego School of Medicine, La Jolla, California.

*These authors contributed equally to this work.

Innovation

Most donor cells do not survive for prolonged periods due to detrimental microenvironment of ischemic myocardium, which limits clinical application of cell-based therapies. Our research suggest for the first time that the liver X receptor (LXR) agonist may serve as a potent agent for protecting transplanted adipose-derived mesenchymal stem cells from inflammation and oxidative stress injury in the infarcted myocardium, and promote their functional survival, thereby enhancing cardiac repair and function. LXR agonist is a promising agent for cell-based therapy clinical translation.

also found that regulating local inflammation in ischemic tissue with sarpegrelate could enhance engrafted AD-MSCs viability and antiapoptotic/proangiogenic efficacy *in vivo* (7). In addition to microenvironmental regulation, increasing the stem cells' ability to resist local stress, such as local inflammation and oxidative stress, is also crucial for stem cell survival and efficacy (22, 37). Therefore, it is imperative to improve the engraftment microenvironment as well as reinforce stem cell biological function to withstand the inhospitable ischemic milieu of the infarcted heart.

Liver X receptors (LXR α and LXR β) are members of the nuclear receptor superfamily that have been recently recognized as novel pharmacological targets for cardiovascular disease therapy (15). LXR α is expressed predominantly in the liver, kidney, intestine, macrophages, and adipose tissue; whereas LXR β is expressed ubiquitously. LXR and LXR ligands have been previously reported to regulate inflammation and immune response (16, 17). Lei *et al.* demonstrated that LXR agonists could attenuate ischemia and reperfusion injury (19). Interestingly, LXR and LXR ligands are also found to modulate the balance between cell survival and death. It is revealed that LXR ligand 24(S), 25-epoxycholesterol (24, 25-EC) promotes embryonic stem cell proliferation, differentiation, and neurogenesis (27, 32). However, the effect of LXR

agonists on AD-MSCs survival and biological behavior remains unclear. The ability of LXR agonist to enhance AD-MSCs functional survival after transplantation into infarct myocardium warrants further investigation.

In this study, we assessed the role of LXR agonist T0901317 in the survival of intramyocardially engrafted mAD-MSCs^{Fluc⁺-eGFP⁺} isolated from Fluc⁺-eGFP⁺ transgenic mice by tracking viable cells longitudinally *in vivo* with noninvasive bioluminescence imaging (BLI). We also further elucidated the mechanism of the LXR agonist's effects through using a hypoxia/serum deprivation (H/SD) cell model *in vitro*. We sought to assess the ability of an LXR agonist to promote the survival of transplanted AD-MSCs *in vivo* and improve cardiac function after myocardial infarction (MI) injury.

Results

Characterization and LXRs expression of AD-MSCs

mAD-MSCs^{Fluc⁺-eGFP⁺} could be abundantly isolated from adipose samples ($\sim 10^6$ cells per gram raw tissues) and exhibited a fibroblastoid morphology *in vitro* (Fig. 1C). Fluorescence microscopy manifested bright enhanced green fluorescence protein (eGFP) expression of mADSCs^{Fluc⁺+GFP⁺} (Fig. 1C). mADSCs^{Fluc⁺+GFP⁺} were positive for MSC markers CD90, CD44 and exhibited low expression of endothelial (CD34) and leukocyte markers (CD45), which represented the potential of differentiating into adipocytes and osteogenic cell lineages, as shown in our previous work (7). Furthermore, real-time quantitative PCR (RT-qPCR) and Western blot analysis revealed that the mRNA and protein expression of LXR α and LXR β were present in mAD-MSCs (Fig. 1D).

Linear correlation between mAD-MSCs^{Fluc⁺-eGFP⁺} number and BLI signal

mAD-MSCs^{Fluc⁺-eGFP⁺} isolated from Fluc⁺-eGFP⁺ transgenic mice uniformly expressed firefly luciferase (Fluc) and GFP. *Ex vivo* bioluminescence images of mAD-MSCs^{Fluc⁺-eGFP⁺} showed a linear relationship between the cell number and BLI

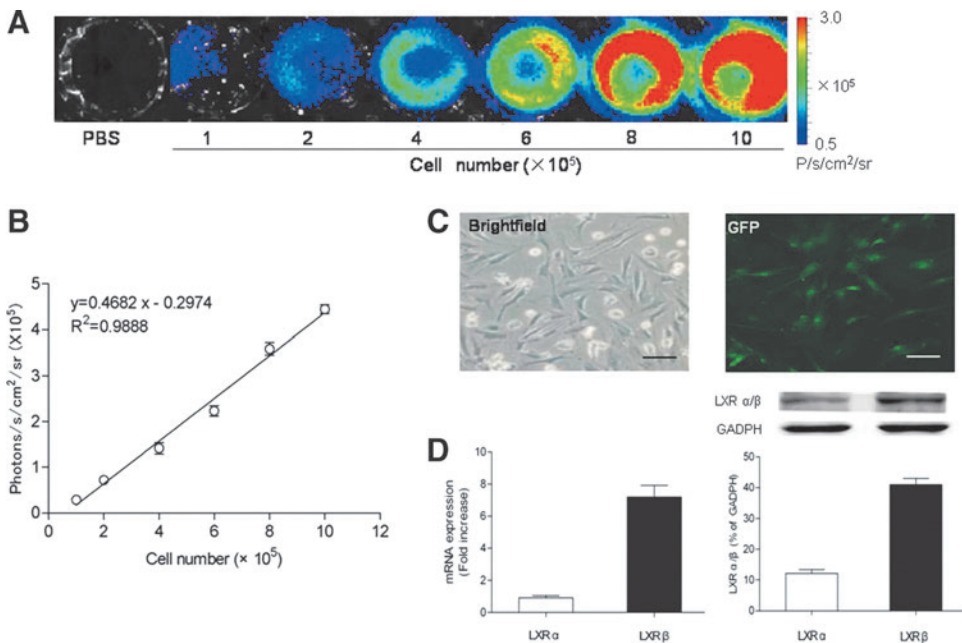


FIG. 1. Morphology and BLI of AD-MSCs *in vitro*. (A) BLI of different numbers of AD-MSCs; (B) The linear relationship between AD-MSCs numbers and BLI signal strength; (C) Morphology of third-passage AD-MSCs cultured *in vitro* ($\times 400$) (left); AD-MSCs is GFP positive (right); (D) mRNA and protein expression of LXR α and LXR β in AD-MSCs ($n = 5$). Scale bar: 10 μ m. AD-MSCs, adipose-derived mesenchymal stem cells; BLI, bioluminescence imaging; LXR, liver X receptor.

signals ($R^2=0.9888$) (Fig. 1A, B). These data indicated that BLI could be used to monitor and quantify transplanted mAD-MSCs^{Fluc+GFP+} in living small animals.

LXR agonist improves the survival of transplanted mAD-MSCs^{Fluc+eGFP+}

To detect the effect of the LXR agonist on the viability of transplanted mAD-MSCs^{Fluc+eGFP+}, BLI was performed during the 4 weeks after mAD-MSCs^{Fluc+eGFP+} transplantation. As shown in Figure 2A and B, there was no significant difference in BLI signal intensity between groups on postoperative day (POD) 2 ($p>0.05$). The signals in both groups decreased gradually in the next few days. However, the BLI signal in the AD-MSCs group declined much more than that in the AD-MSCs+LXR group (on POD 7, AD-MSCs: $1.28 \pm 0.08 \times 10^5$ average photons per second per cm square per steradian [photons/s/cm²/sr] vs. AD-MSCs+LXR: $1.60 \pm 0.11 \times 10^5$ photons/s/cm²/sr, $p<0.05$; on POD 28, AD-MSCs: $0.05 \pm 0.03 \times 10^5$ photons/s/cm²/sr vs. AD-MSCs+LXR: $0.27 \pm 0.05 \times 10^5$ photons/s/cm²/sr, $p<0.05$).

Further *ex vivo* confocal fluorescence microscopy confirmed that more GFP positive engrafted cells could be found in the heart tissue of mice in the AD-MSCs+LXR group than in the AD-MSCs group (ratio of GFP⁺/DAPI: $10.56\% \pm 1.38\%$ vs. $3.94\% \pm 0.61\%$, $p<0.05$) (Fig. 2C).

Combined therapy of AD-MSCs and LXR agonist improves cardiac function after MI

Echocardiography analysis indicated that there was no significant difference in left ventricular ejection fraction

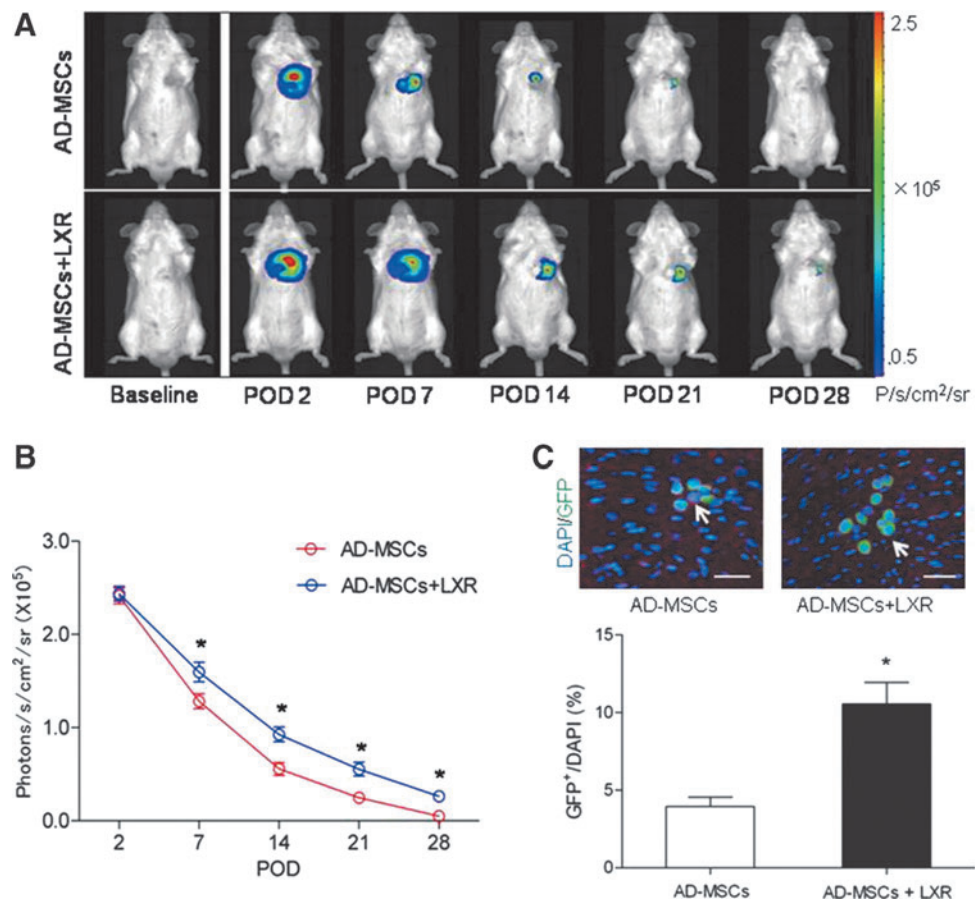
(LVEF) and fraction shortening (FS) between all groups at baseline ($p>0.05$). On POD 2, LVEF significantly decreased in all groups. However, combined therapy of AD-MSCs and LXR improved cardiac function significantly more than expected. Specifically, by POD 7, 14, and 28, LVEF was improved in the combined therapy group compared with MI groups ($p<0.05$). Similarly, FS was significantly improved in the combined therapy group on POD 7, 14, and 28 in contrast to MI groups ($p<0.05$). However, pretreated AD-MSCs with LXR agonist before transplantation could not ameliorate LVEF and FS of MI mice on POD 7, 14, and 28, compared with the MI group ($p>0.05$). Furthermore, combined therapy of LXR agonist and AD-MSCs transfected with Nrf-2 siRNA markedly decreased LVEF and FS on POD 7, 14, and 28, in contrast to the AD-MSCs+LXR group ($p<0.05$) (Fig. 3A, B).

Combined therapy of AD-MSCs and LXR agonist inhibits cardiomyocyte apoptosis and reduces infarcted area size after MI

TUNEL assay showed that the apoptotic index (AI) was significantly higher in mice undergoing MI than in mice undergoing sham operation ($21.8\% \pm 1.46\%$ vs. $3.9\% \pm 0.24\%$, $p<0.01$). Unexpectedly, AD-MSC administration alone did not significantly decrease AI compared with the MI group ($p>0.05$). In contrast, combination therapy of AD-MSCs+LXR significantly lowered AI compared with that in the MI group ($11.0\% \pm 0.64\%$ vs. $21.8\% \pm 1.46\%$, $p<0.05$) (Fig. 3C, D).

FIG. 2. BLI of transplanted AD-MSCs.

(A) To assess longitudinal transplanted AD-MSCs survival, animals were imaged for 4 weeks. Bioluminescence signals were detected in AD-MSCs+LXR group mice at day 2, 7, 14, 21, and 28, although in the AD-MSCs group bioluminescence signal is not detected at day 28; (B) Quantification of imaging signals showed that bioluminescence signals in the AD-MSCs+LXR group are much higher than those in AD-MSCs group ($n=5$). $*p<0.05$; (C) GFP-positive cells (white arrow) were hardly found in the heart of the AD-MSCs group mice, but in AD-MSCs+LXR group mice, GFP-positive cells were occasionally found ($n=3$). $*p<0.05$, Scale bar: 10 μ m.



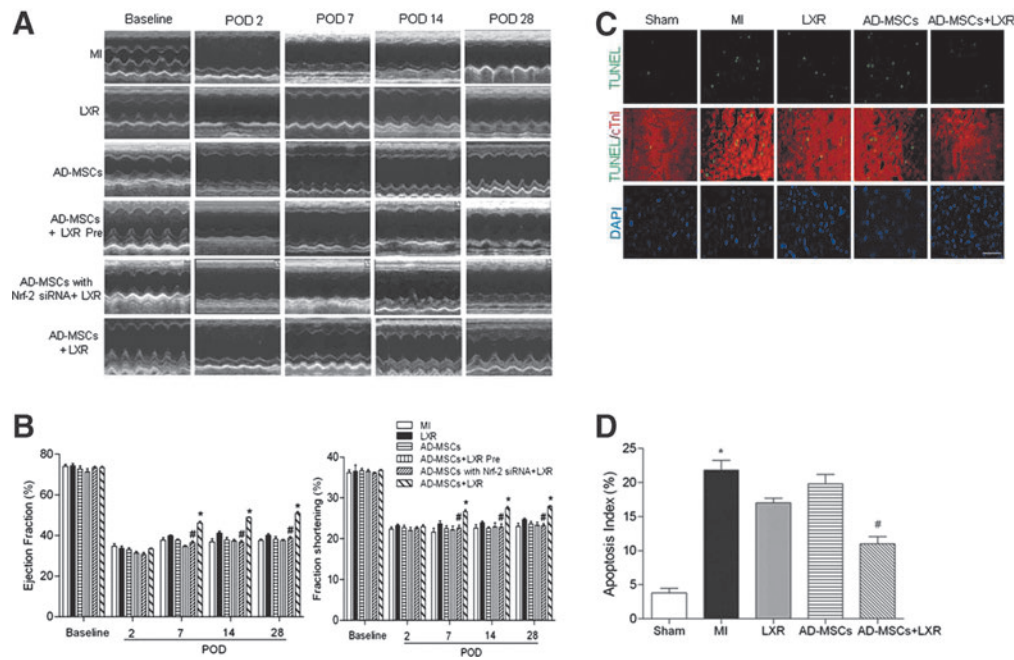


FIG. 3. Cardiac function and cardiomyocyte apoptosis after infarction. (A) Representative M-mode echocardiographic data of infarcted hearts receiving phosphate-buffered saline, AD-MSCs, AD-MSCs+LXR Pre, AD-MSCs with Nrf-2 siRNA+LXR, and AD-MSCs+LXR at POD 2, 7, 14, and 28; (B) Comparison of fractional shortening and ejection fraction between all groups, respectively ($n=5$). $*p<0.05$ versus MI group, $^{\#}p<0.05$ versus AD-MSCs+LXR group; (C) Representative photographs of TUNEL-stained myocardial sections from each group at POD 3. The images show TUNEL-positive cells (green fluorescence), myocardium stained with monoclonal antibody cTnI (red fluorescence), and DAPI-positive nuclei (blue fluorescence); (D) Graphs summarize the number of TUNEL-positive nuclei per 100 nuclei and present the average from five different fields randomly selected ($\times 100$ magnification) ($n=5$). $*p<0.01$ versus sham group, $^{\#}p<0.05$ versus MI group. Scale bar: $50\ \mu\text{m}$. DAPI, 4',6-diamidino-2-phenylindole; MI, myocardial infarction; POD, postoperative days.

Masson's trichrome staining revealed that although the area of myocardial infarcted size was not significantly reduced in the AD-MSC group compared with that in the MI group ($42.09\% \pm 1.30\%$ vs. $53.15\% \pm 1.22\%$, $p>0.05$), it was substantially lower in the AD-MSCs+LXR group than in the MI group ($26.30\% \pm 1.70\%$ vs. $53.15\% \pm 1.22\%$, $p<0.05$). However, AD-MSCs engraftment with LXR agonist pretreated could not reduce myocardial infarcted area size, in contrast to the MI group ($p>0.05$). In addition, combined therapy of LXR agonist and AD-MSCs transfected with Nrf-2 siRNA was found to increase myocardial infarcted area size on POD 28, compared with AD-MSCs+LXR group ($p<0.05$) (Fig. 4A).

Combined therapy of AD-MSCs and LXR agonist increases capillary density in the peri-infarcted area

Immunohistochemical staining of CD31-positive tubular structures showed that capillary density markedly increased in the peri-infarcted area of the AD-MSCs+LXR group than that in the MI group ($p<0.05$). However, almost no CD31-positive vessels were observed in sham group (Fig. 4B).

Combined therapy of AD-MSCs and LXR agonist regulates inflammatory cytokine, reactive oxygen species, and growth factor production

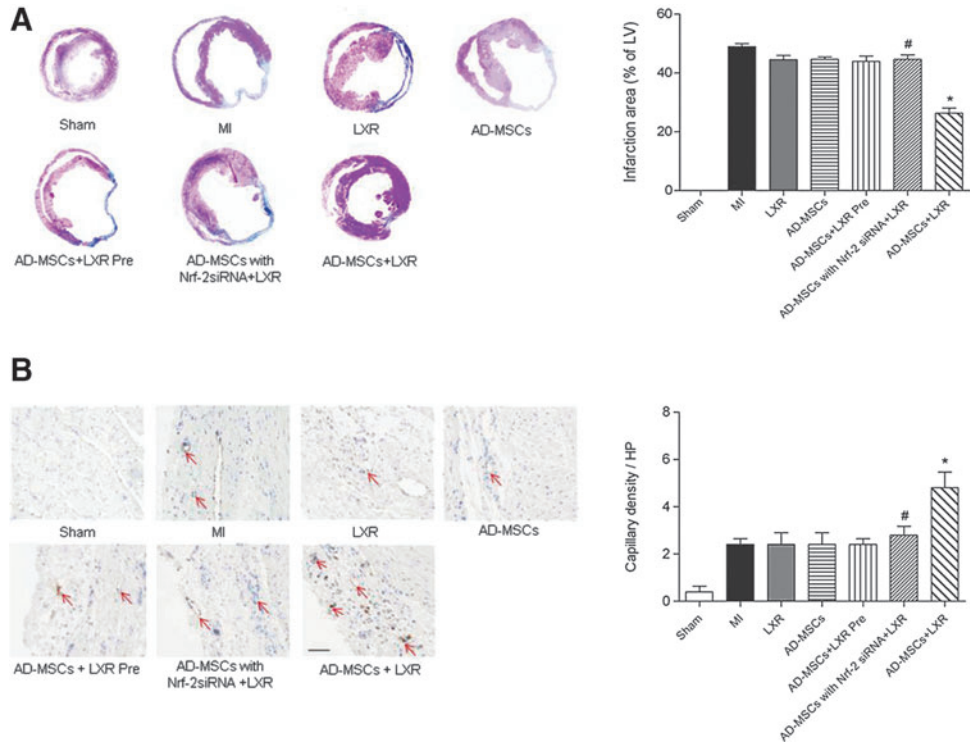
ELISA analysis revealed that MI led to a significant increase of tumor necrosis factor- α (TNF- α), and interleukin-6 (IL-6) in injured myocardium, compared with animals undergoing sham operation (TNF- α : 24.31 ± 0.98 pg/mg protein

vs. 5.20 ± 0.45 pg/mg protein; IL-6: 19.21 ± 1.31 pg/mg protein vs. 4.57 ± 0.34 pg/mg protein, $p<0.01$). However, administration of the LXR agonist prevented the increase of TNF- α and IL-6 in infarcted myocardium (TNF- α : 17.94 ± 1.28 pg/mg protein vs. 24.31 ± 0.98 pg/mg protein; IL-6: 12.14 ± 1.02 pg/mg protein vs. 19.21 ± 1.31 pg/mg protein, $p<0.05$). Surprisingly, AD-MSCs alone did not exert a dramatic effect on TNF- α and IL-6 levels in injured myocardium ($p>0.05$) (Fig. 5A, B).

Previous research has demonstrated that reactive oxygen species (ROS) generated in infarcted myocardium stimulates cardiomyocyte apoptosis (21) and decreases AD-MSCs survival after engraftment (38). Therefore, ROS generation was assessed in our experimental model using dihydroethidium (DHE) fluorescence. The LXR agonist significantly lowered the MI-induced increase of DHE fluorescence intensity ($p<0.05$). Engrafted AD-MSCs alone did not influence DHE fluorescence intensity as compared with the MI group ($p>0.05$) (Fig. 5E).

ELISA analysis revealed that combined therapy with AD-MSCs and LXR significantly elevated plasma levels of vascular endothelial growth factor (VEGF) and basic fibroblast growth factor (bFGF), in contrast to the MI group (VEGF: 255.82 ± 6.49 pg/mg protein vs. 174.24 ± 6.08 pg/mg protein, $p<0.05$; bFGF: 404.03 ± 6.98 pg/mg protein vs. 320.8 ± 7.64 pg/mg protein, $p<0.05$). Nevertheless, plasma levels of VEGF and bFGF were not increased when mice received treatment with AD-MSCs or LXR alone ($p>0.05$) (Fig. 5C, D).

FIG. 4. Myocardial infarct size, fibrosis, and angiogenesis after infarction. (A) Masson's trichrome-stained myocardial sections and comparison of fibrosis areas in a subgroup of animals at POD 28 ($n=5$). $*p<0.05$ versus MI group, $^{\#}p<0.05$ versus AD-MSCs+LXR group; (B) Representative photographs of CD31-positive vessel (Red arrow) and quantification analysis from each group ($\times 200$ magnification) ($n=5$). $*p<0.05$ versus MI group, $^{\#}p<0.05$ versus AD-MSCs+LXR group. Scale bar: 100 μm .



LXR agonist protects AD-MSCs from H/SD injury

To determine the protective effects of the LXR agonist on viability during H/SD injury, AD-MSCs were exposed to various doses of LXR agonist (1, 5, 10, and 15 μM) for 24 h,

followed by H/SD injury for 6 h. Cell viability was analyzed by BLI. Results revealed that AD-MSC viability was significantly hindered by H/SD injury ($1.7 \pm 0.085 \times 10^5$ photons/s/cm²/sr vs. $4.5 \pm 0.029 \times 10^5$ photons/s/cm²/sr, $p<0.01$). However, 10 μM of LXR agonist efficiently blocked the decreased

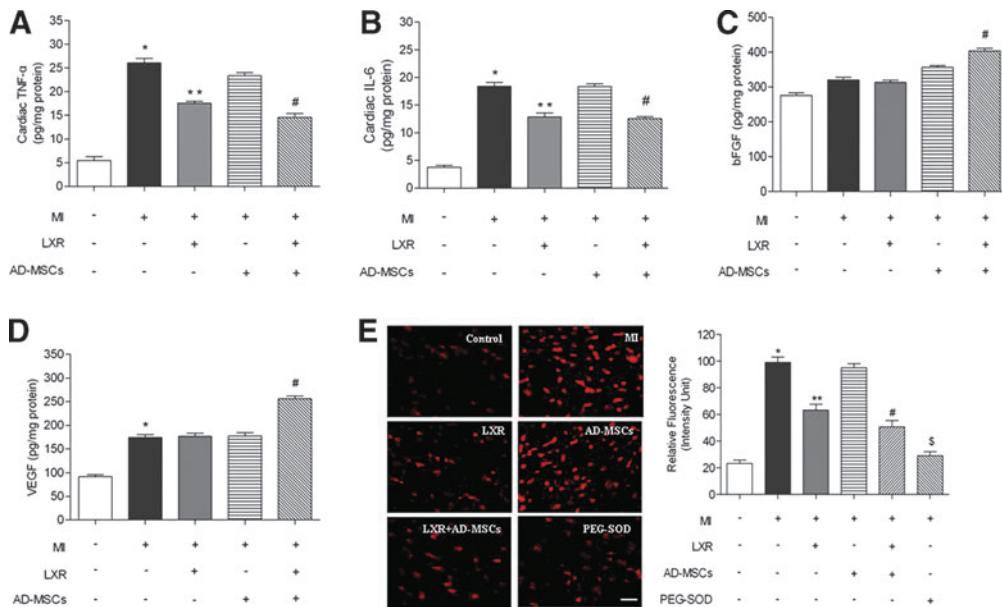


FIG. 5. Effects of LXR agonist and AD-MSCs on MI-induced inflammatory factors, growth factors, and ROS generation. (A, B) LXR agonists reduced cardiac levels of TNF- α and IL-6 in MI+LXR and MI+LXR+AD-MSCs groups compared with the MI group ($n=5$). $*p<0.01$ versus Sham group, $**p<0.05$ versus MI group, $^{\#}p<0.05$ versus MI group; (C, D) LXR agonists decrease serum levels of bFGF and VEGF in MI+LXR+AD-MSCs group compared with MI group ($n=5$). $^{\#}p<0.05$ versus sham group; (E) Representative images of dihydroethidium fluorescence staining that evaluated ROS generation in myocardium and bar graph summarizing fluorescence intensity ($n=5$). $*p<0.01$ versus Sham group, $**p<0.05$ versus MI group, $^{\#}p<0.05$ versus MI group, and $^s p<0.05$ versus MI group. Scale bar: 50 μm . bFGF, basic fibroblast growth factor; IL-6, interleukin-6; ROS, reactive oxygen species; TNF- α , tumor necrosis factor- α ; VEGF, vascular endothelial growth factor.

AD-MSCs viability despite H/SD injury ($1.7 \pm 0.085 \times 10^5$ photons/s/cm²/sr vs. $3.32 \pm 0.13 \times 10^5$ photons/s/cm²/sr, $p < 0.05$) (Fig. 6A, B). Then, to assess the anti-apoptotic role of the LXR agonist ($10 \mu\text{M}$) on AD-MSCs after H/SD injury, flow cytometry analysis was performed. Results showed that H/SD injury greatly increased the percentage of apoptotic AD-MSCs ($18.16\% \pm 0.68\%$ vs. $4.52\% \pm 0.19\%$, $p < 0.01$), whereas LXR agonist treatment partially inhibited H/SD-induced AD-MSCs apoptosis ($10.60\% \pm 0.58\%$ vs. $18.16\% \pm 0.69\%$, $p < 0.01$).

Furthermore, Nrf-2 siRNA intervention could block decreased apoptosis of AD-MSCs induced by LXR agonist ($14.76\% \pm 0.58\%$ vs. $10.60\% \pm 0.58\%$, $p < 0.05$) (Fig. 6C, D).

LXR agonist modulates inflammatory cytokine and growth factor secretion in AD-MSCs injured by H/SD

Analysis of the inflammatory cytokine composition of AD-MSC supernatants showed that the concentration of TNF- α and IL-6 secreted by AD-MSCs was significantly higher in the H/SD group than in the control group (TNF- α : 21.90 ± 0.80 pg/ml vs. 7.34 ± 0.39 pg/ml, $p < 0.01$; IL-6: 0.88 ± 0.02 ng/ml vs. 0.25 ± 0.02 ng/ml, $p < 0.01$, respectively). Nevertheless, addition of the LXR agonist significantly decreased the secretion of TNF- α and IL-6 by AD-MSCs compared with the H/SD group (TNF- α : 21.90 ± 0.80 pg/ml vs. 11.48 ± 0.38 pg/ml, $p < 0.05$; IL-6: 0.88 ± 0.02 ng/ml vs. 0.52 ± 0.02 ng/ml, $p < 0.05$). Transfection with Nrf-2 siRNA could inhibit LXR agonist's effect of lowering TNF- α and IL-6 secretion (TNF- α : 18.36 ± 0.86 pg/ml vs. 11.48 ± 0.38 pg/ml,

$p < 0.05$; IL-6: 0.85 ± 0.05 ng/ml vs. 0.52 ± 0.02 ng/ml, $p < 0.05$) (Fig. 7A). Analysis of the growth factor composition of AD-MSC supernatants indicated that the levels of VEGF and bFGF were much higher in the H/SD group than that in the control group (VEGF: 4.39 ± 0.35 ng/ml vs. 1.98 ± 0.22 ng/ml, $p < 0.05$; bFGF: 18.61 ± 2.43 ng/ml vs. 8.67 ± 0.97 ng/ml, $p < 0.05$), and that there was no major difference between H/SD group, LXR agonist-treated group, and Nrf-2 siRNA intervention group ($p > 0.05$) (Fig. 7B).

LXR agonist attenuates intracellular and mitochondrial ROS production in AD-MSCs after H/SD injury

The fluorescence intensity of dichlorofluorescein (DCF) was increased in H/SD group compared with that in the control group ($p < 0.01$). LXR agonist treatment significantly lowered the mean fluorescence intensity ($p < 0.05$), suggesting that the LXR agonist decreased ROS production in H/SD-injured AD-MSCs. Furthermore, Nrf-2 siRNA could reverse this effect of LXR agonist ($p < 0.05$) (Fig. 7C). Likewise, LXR agonist attenuated H/SD-induced mitochondrial ROS generation, as indicated by the DCF mean fluorescence intensity ($p < 0.05$). However, Nrf-2 siRNA abolished the inhibitory effect of LXR agonist in regulating ROS generation ($p < 0.05$) (Fig. 7D). Interestingly, NADPH oxidase subunits gp91^{phox} expression was significantly increased under H/SD condition, which was reversed by LXR agonist treatment ($p < 0.01$). However, Nrf-2 siRNA intervention partly abrogated the roles of LXR agonist in gp91^{phox}

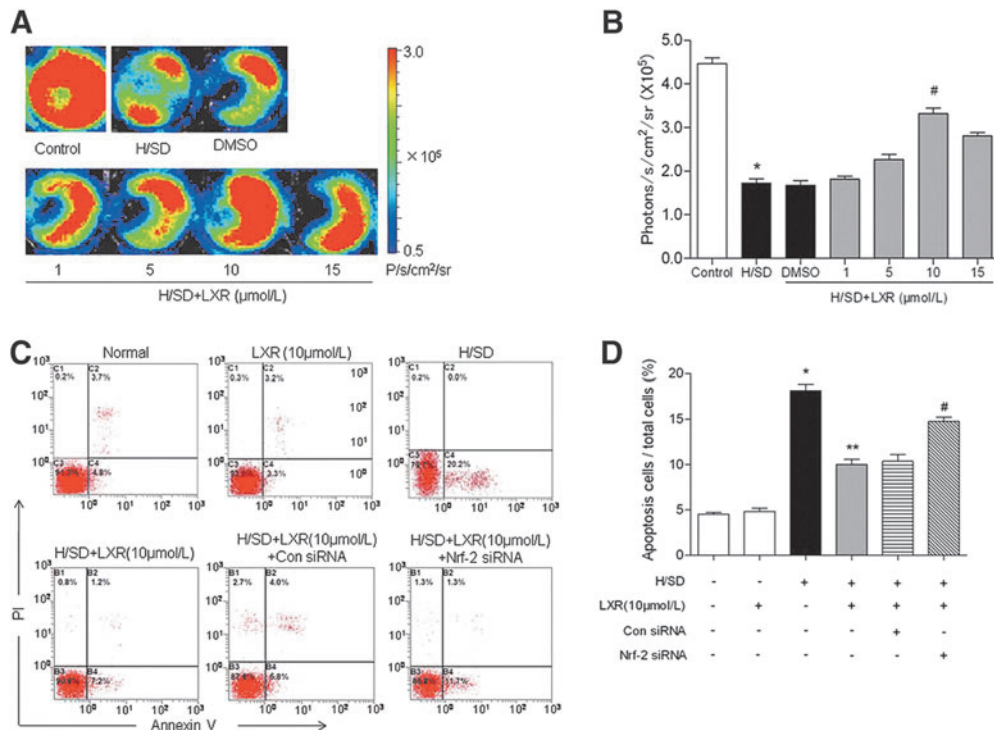


FIG. 6. The effect of the LXR agonist on AD-MSCs survival and apoptosis after H/SD injury. (A) BLI of AD-MSCs undergoing H/SD injury with DMSO or different concentrations of LXR agonist treatment; normal condition AD-MSCs is used as control; (B) Comparison of fluorescence average radiance of AD-MSCs in different groups ($n = 5$). * $p < 0.01$ versus control, # $p < 0.05$ versus H/SD group; (C) Apoptosis was analyzed by flow cytometry after staining with Annexin V and PI; (D) Quantification analysis of the apoptotic AD-MSCs was presented as the percentage of apoptotic cells ($n = 5$). * $p < 0.01$ versus control, ** $p < 0.01$ versus H/SD group, and # $p < 0.05$ versus H/SD+LXR group. DMSO, dimethyl sulfoxide; H/SD, hypoxia/serum deprivation; PI, propidium iodide.

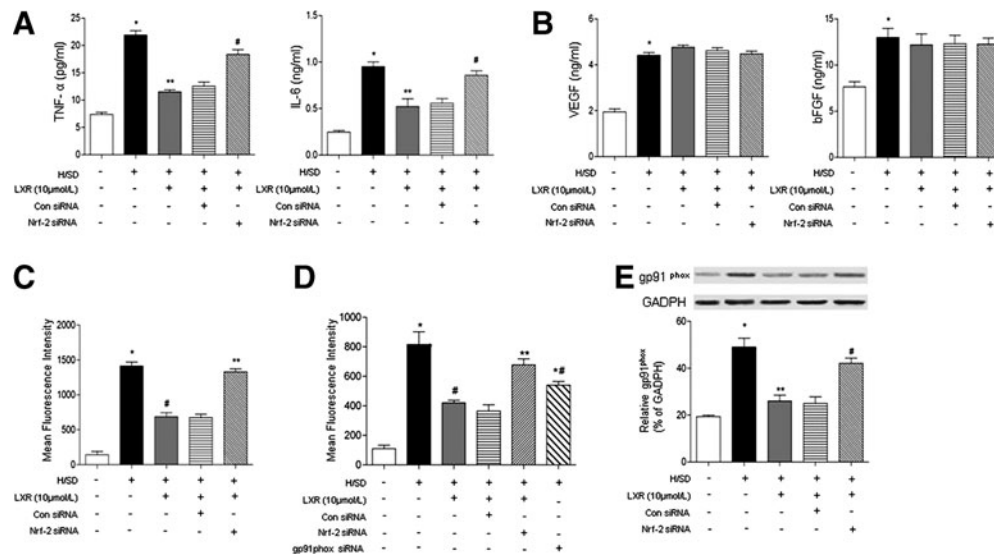


FIG. 7. Effect of LXR agonists on inflammatory cytokine, growth factor secretion, and intracellular and mitochondrial ROS generation of AD-MSCs under hypoxic conditions. (A) Concentration of TNF- α and IL-6 released by AD-MSC was measured by ELISA ($n=5$). * $p < 0.01$ versus control, ** $p < 0.05$ versus H/SD group, and # $p < 0.05$ versus H/SD+LXR group; (B) Concentration of VEGF and bFGF secreted by AD-MSCs was also detected by ELISA ($n=5$). * $p < 0.05$ versus control group; (C) Quantification analysis of intracellular DCF fluorescence intensity in AD-MSCs ($n=5$); (D) Quantification analysis of mitochondrial DCF fluorescence intensity in AD-MSCs ($n=5$). * $p < 0.01$ versus control, ** $p < 0.05$ versus H/SD group, # $p < 0.05$ versus H/SD+LXR group, and **# $p < 0.05$ versus H/SD group; (E) NADPH oxidase subunits gp91^{phox} expression was measured by Western blotting analysis ($n=5$). * $p < 0.01$ versus control, ** $p < 0.01$ versus H/SD group, and # $p < 0.05$ versus H/SD+LXR group. DCF, dichlorofluorescein.

expression ($p < 0.05$) (Fig. 7E). In addition, depletion of gp91^{phox} with siRNA could inhibit H/SD-induced mitochondrial ROS production ($p < 0.05$) (Fig. 7D).

LXR agonist inhibits TLR4/NF- κ B signaling pathway activation in AD-MSCs injured by H/SD or oxidative stress

To determine the role of the TLR4/NF- κ B signaling pathway in LXR agonist protection of AD-MSCs from H/SD injury, the expression or phosphorylation levels of TLR4, MyD88, TRAF-6, I κ B α , and NF- κ B-p65 in AD-MSCs was detected by Western blot. The expression of TLR4, MyD88, and TRAF-6 significantly increased under H/SD conditions ($p < 0.01$), whereas the change was reversed by pretreatment with 10 μ M of LXR agonist ($p < 0.05$). However, knockdown Nrf-2 by siRNA significantly inhibited the LXR agonist's effects in modulating TLR4, MyD88, and TRAF-6 expression ($p < 0.05$). Consistent with these results, phosphorylation levels of I κ B α were also markedly elevated in the H/SD group in comparison with the control group ($p < 0.01$), and pretreatment with 10 μ M LXR agonist inhibited I κ B α phosphorylation ($p < 0.05$). Similarly, NF- κ B-p65 protein expression was significantly increased in the H/SD group compared with the control group ($p < 0.01$), and 10 μ M of the LXR agonist reversed the increase of NF- κ B-p65 protein expression ($p < 0.01$). Nevertheless, Nrf-2 siRNA treatment also reversed the LXR agonist's inhibition of I κ B α phosphorylation and NF- κ B-p65 protein expression ($p < 0.05$) (Fig. 8 and Supplementary Fig. S1; Supplementary Data are available online at www.liebertpub.com/ars).

Western blot analysis also revealed that the expression of TLR4, MyD88, TRAF-6, and NF- κ B-p65 protein as well as

phosphorylation levels of I κ B α were significantly elevated under oxidative stress condition ($p < 0.01$). However, 10 μ M of LXR agonist could downregulate these proteins' increased expression or phosphorylation levels induced by oxidative stress injury ($p < 0.01$). Further, Nrf-2 siRNA knockdown partly abolished the roles of LXR agonist in regulating the TLR4/NF- κ B pathway ($p < 0.05$) (Fig. 9 and Supplementary Fig. S1).

The LXR agonist upregulates the Keap-1/Nrf-2 signaling pathway in AD-MSCs under H/SD or oxidative stress conditions

Our results showed that compared with the H/SD groups, Keap-1 protein expression was significantly decreased in the H/SD+LXR group ($p < 0.01$). Simultaneously, Nrf-2 protein level was decreased in the cytoplasm and increased in the nucleus in the H/SD+LXR group ($p < 0.01$), indicating that LXR administration promoted nuclear translocation of the Nrf-2 protein after H/SD injury. In addition, the level of HO-1 protein markedly rose in the LXR+H/SD group compared with the control group ($p < 0.01$), but not in the H/SD group. Furthermore, treatment with the NF- κ B-p65 siRNA also significantly increased Nrf-2 protein translocation and HO-1 protein expression in contrast to the control group ($p < 0.05$) (Fig. 8 and Supplementary Fig. S1).

In addition, LXR agonist markedly attenuated Keap-1 protein expression after H₂O₂-stimulated oxidative stress injury, and it also boosted Nrf-2 protein translocation and HO-1 protein expression ($p < 0.05$). Similarly, NF- κ B-p65 siRNA pretreatment also upregulated Nrf-2 protein translocation and HO-1 protein expression after oxidative stress injury ($p < 0.05$) (Fig. 9 and Supplementary Fig. S1).

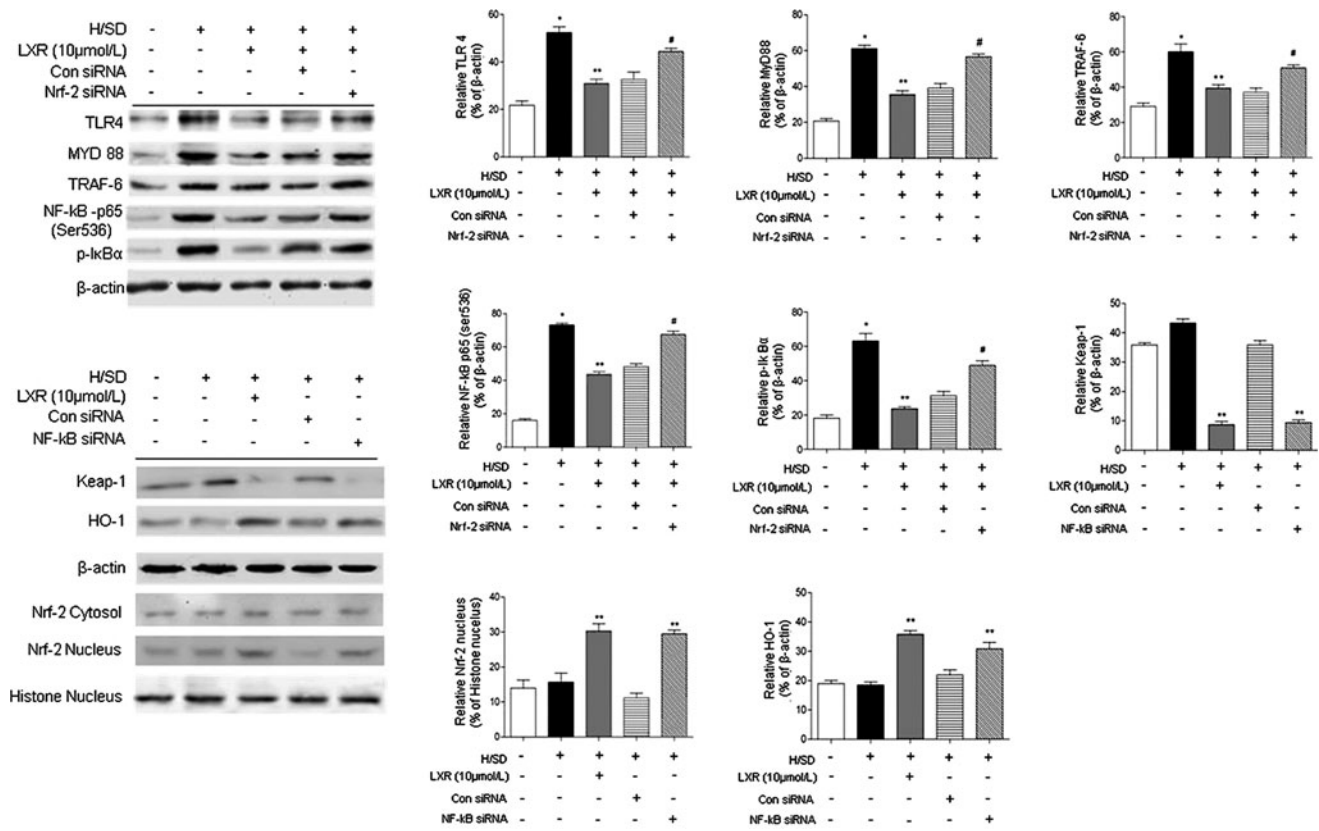


FIG. 8. The protein expression of TLR4, MyD88, TRAF-6, and NF-κB-p65; phosphorylation of IκBα, Keap-1, and Nrf-2 in AD-MSCs under H/SD condition were determined by Western blotting ($n=5$, * $p < 0.05$ versus control, ** $p < 0.05$ versus H/SD group, and # $p < 0.05$ versus H/SD+LXR group).

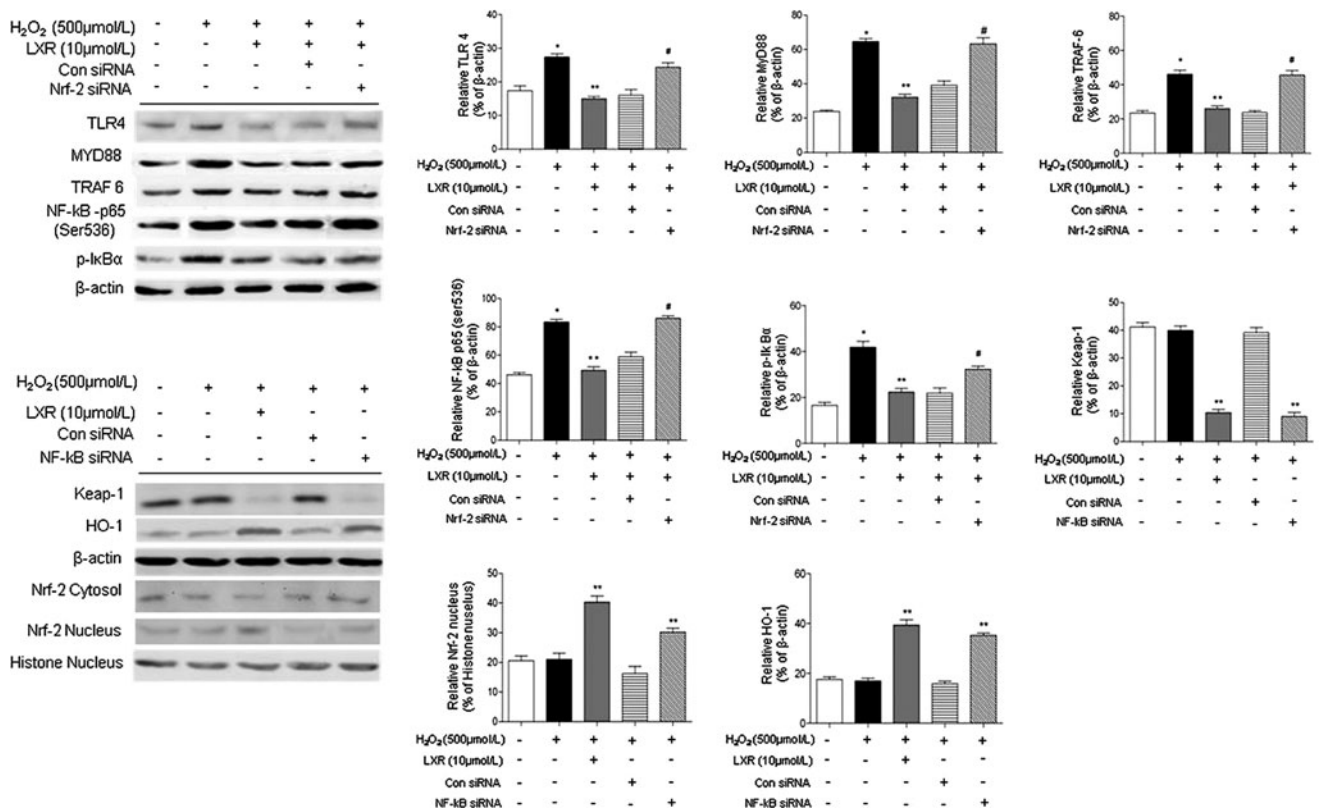


FIG. 9. The protein expression of TLR4, MyD88, TRAF-6, and NF-κB-p65; phosphorylation of IκBα, Keap-1, and Nrf-2 in AD-MSCs under H₂O₂-stimulated oxidative stress condition were determined by Western blotting ($n=5$, * $p < 0.05$ versus control, ** $p < 0.05$ versus H₂O₂ group, and # $p < 0.05$ versus H₂O₂+LXR group).

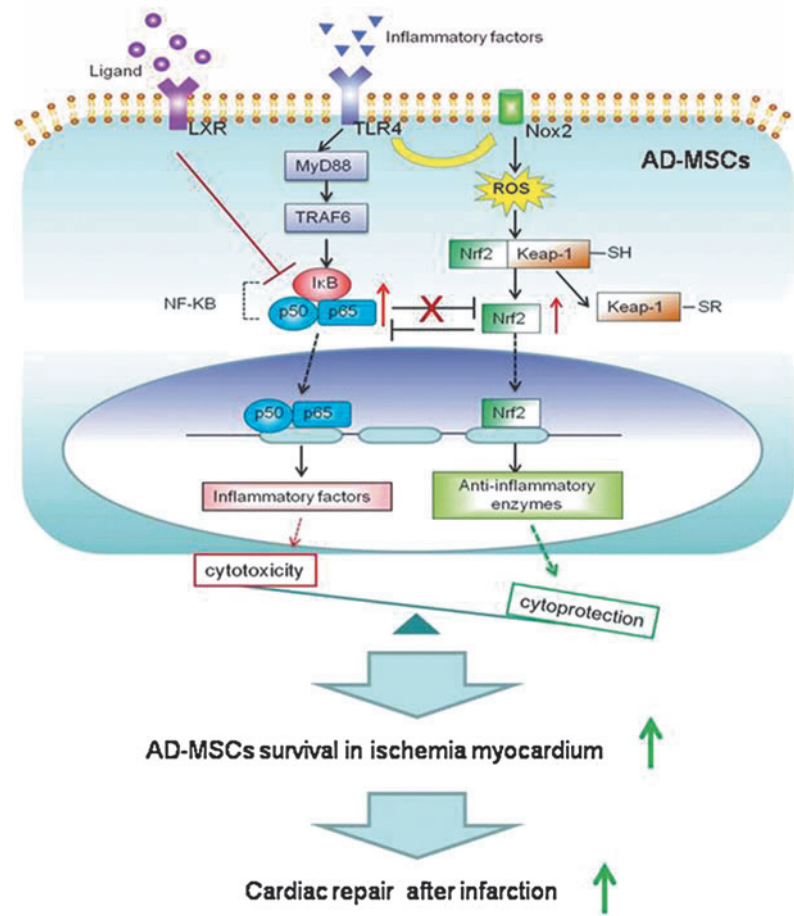


FIG. 10. Proposed scheme for mechanisms of promoting AD-MSCs survival in ischemia myocardium by LXR agonist.

Discussion

Enhanced survival of transplanted stem cells is crucial for current cell-based therapies. Most donor cells do not survive for prolonged periods in ischemic myocardium, which limits clinical application of cell-based therapies (25). Some recent studies show that inflammation and oxidative stress are major contributors to the acute death of engrafted stem cells (34, 36). Our previous work also reveals that inflammation in the ischemic hind limb inhibits functional survival of mADSCs *in vivo* (6). Thus, seeking effective targets to ameliorate inflammation in the host microenvironment after ischemic injury is an important part of promoting donor cell survival and cardiac repair.

Recently, investigators have found that LXR activation modulates inflammation and inhibits ischemic injury (23, 29). However, whether LXR activation enhances engrafted cell survival remains uncertain. In the present study, we found that combined therapy with LXR agonist T0901317 and AD-MSCs attenuated myocardial infarct size and improved myocardial function after infarction due to the protective effects of the LXR agonist on the functional survival of AD-MSCs after transplantation. Putative mechanisms may involve the anti-oxidative stress and anti-inflammatory effects of LXR on the myocardial microenvironment and AD-MSCs *via* modulation of the TLR4/NF-κB and Keap-1/Nrf-2 signaling pathways.

To clarify this, we used BLI to track engrafted AD-MSCs and showed that most of the implanted AD-MSCs underwent acute cell death in the infarcted myocardium within 7

days, which was similar with prevailing research (41). Our previous studies also found that a higher dosage of stem cells could not avoid acute loss and apoptosis after delivery (2). Furthermore, echocardiography demonstrated that transplantation of AD-MSCs after AMI did not significantly improve cardiac function. These data indicated that poor viability and severe apoptosis impaired the therapeutic effect of the transplanted AD-MSCs.

LXRs are known as regulators of glucose, lipid, and cholesterol metabolism. Many previous studies have suggested that LXR activation regulates inflammation and immune response (10). Recently, LXR ligands were reported to be involved in modulating the balance between embryonic stem cell survival and differentiation, as well as promoting neurogenesis (27, 32). To investigate the role of LXR in cell survival, we compared BLI signal intensity in mice receiving AD-MSCs alone and combined therapy that included an LXR agonist. The data indicate that LXR agonist treatment enhances the survival of AD-MSCs after engraftment. However, pretreatment AD-MSCs with LXR agonist before transplantation is not sufficient to enhance the therapeutic potential of engrafted cells. Previous work has already revealed that the microenvironment around stem cells plays a critical role in cell survival and function (14). High levels of pro-inflammatory factors and ROS, two strong components of host response to injury, will retard stem cell survival and decrease their regenerative capabilities (6, 18, 30, 33). When we measured inflammatory cytokine (TNF-α and IL-6) and

ROS levels in tissue, we found that an LXR agonist could decrease TNF- α , IL-6, and ROS generation in ischemically injured myocardium, providing a better local microenvironment that was crucial to increased AD-MSC survival. In addition to microenvironmental modulation, important stem cell properties affecting survival and function, such as paracrine secretion and differentiation, may be altered by ischemic injury (20). ELISA and DCF fluorescence intensity assays showed that an LXR agonist could significantly decrease TNF- α , IL-6, and ROS levels produced by AD-MSCs under hypoxic condition, although it did not affect growth factors (e.g., VEGF and bFGF) levels which were elevated in response to hypoxic stimuli. In addition, it is recognized that NADPH oxidase subunit gp91^{phox} contributes to mitochondrial ROS production through activation of redox-sensitive PKC ϵ and the opening of mitoK_{ATP} (5a). Our data support the hypothesis that LXR agonist attenuates the inflammatory response in AD-MSCs under hypoxic conditions, and prevents oxidative stress induced by hypoxia injury through decreasing gp91^{phox} expression.

As for the differentiation ability of transplanted AD-MSCs, our previous studies showed that transplanted MSCs rarely differentiated into cardiomyocytes *in vivo* (7, 41). Other literature put forward the debate of whether implanted MSCs possess beneficial multipotent differentiation ability in infarcted myocardium (1). Based on these findings, cardiac functional benefits of MSCs transplantation may not be mainly attributable to cells' differentiation. Therefore, we placed more emphasis on whether the LXR agonist has any effect or not on MSCs paracrine capacity in this research. Masson's staining and CD31 immunohistochemical staining also indicated that cell engraftment therapy exerts cardioprotective roles mainly through paracrine mechanism.

Furthermore, previous studies revealed that oxidative stress and inflammation played essential roles in pathogenesis of cardiac remodeling. ROS had been implicated to promote cardiac remodeling through regulating matrix metalloproteinase expression or cytokines and growth factors signaling pathway (3, 5, 24). In addition, inflammation is also reported to mediate initiation and development of cardiac fibrosis (35). In this study, we observed that LXR agonist significantly attenuated inflammation and oxidative stress in the myocardium after MI. Thus, it can be inferred that combined therapy of AD-MSCs and LXR agonist protects against cardiac remodeling through inhibiting inflammation and oxidative stress.

It is well recognized that NF- κ B regulates at least three inflammation-related genes and that its activation exerts varied effects on cell apoptosis, survival, and autophagy (9). Recent data have shown that regulating inflammation in AD-MSCs can enhance their viability by inhibiting the TLR4/NF- κ B signaling pathway (40). Therefore, we clarified whether the TLR4/MyD88/NF- κ B signaling pathway was mechanistically implicated in the LXR agonist's cytoprotective effects. Interestingly, the AD-MSC *in vitro* assay results suggest that the LXR agonist promotes AD-MSC survival and inhibits proinflammatory cytokine production in AD-MSCs after ischemic injury, at least partly, by negatively regulating the TLR4/MyD88/NF- κ B signaling pathway.

The Keap-1/Nrf-2 system has been recognized as a cellular endogenous defense mechanism against oxidative stress (4, 12). However, it was unknown whether the Keap-1/Nrf-2 signaling pathway influenced AD-MSCs viability, function,

or ability to withstand ROS damage under stressful conditions. Western blot results suggest that the LXR agonist activates Keap-1/Nrf-2 signaling and promotes Nrf-2 nuclear translocation. Knockdown of Nrf-2 with siRNA could partly abrogate the protective roles of LXR agonist in promoting stem cell survival, reducing inflammatory cytokines and ROS generation as well as downregulating TLR4/MyD88/NF- κ B signaling pathway in AD-MSCs under H/SD condition. Our research also confirmed that Nrf-2 silencing abolished protective roles of LXR in engrafted AD-MSCs *in vivo*. Based on the *in vivo* and *in vitro* experiment results, it can be concluded that although the LXR agonist partly ameliorated myocardial microenvironment after MI, Nrf-2 silencing of AD-MSCs would attenuate cells' ability to resist inflammation and oxidative stress, which might abrogate direct and indirect protective effects of LXR agonist on AD-MSCs *in vivo*. In addition, we used siRNA to inhibit NF- κ B-p65 expression, and demonstrated that NF- κ B-p65 siRNA-mediated inhibition significantly increased the expression of Nrf-2 and HO-1, and decreased the expression of Keap-1. Based on these results, we could infer that the endogenous Keap-1-Nrf-2 system of AD-MSCs was repressed by NF- κ B activation under ischemic injury-induced oxidative stress conditions, but an LXR agonist can downregulate TLR4/MyD88/NF- κ B and reactivate Keap-1/Nrf-2/HO-1 pathway of AD-MSCs to resist the oxidative stress (Fig. 10). However, other complementary mechanisms related to LXR agonist may also be involved in activating the Keap-1-Nrf-2 signaling pathway, which is needed to be further elucidated.

Despite the relevance of our findings, our study has many limitations. For instance, BLI is not suitable thus far for clinical application because of photon attenuation and scattering limiting detection depth. Second, bioluminescence signal *in vivo* reaches its peak value at \sim 24 h after cell injection, and therefore any information about cell viability within the first 24 h is lost, although presumably a very significant amount of cell loss occurs during this period. Third, we did not use the LXR antagonist to further validate the protective effects of LXR agonist on AD-MSCs, for there was no commercial available LXR antagonist.

In conclusion, our *in vivo* studies showed that the administration of an LXR agonist might effectively enhance the viability of AD-MSCs transplanted into infarcted hearts. The combination treatment of an LXR agonist and AD-MSCs may have a synergistic effect on cardiac functional improvement. In addition, our *in vitro* studies demonstrated that the cytoprotective effect of LXR agonist on AD-MSCs injured by H/SD involves modulation of the TLR4/NF- κ B and Keap-1/Nrf-2 signaling pathways. Therefore, the LXR agonist may serve as a potent agent for protecting transplanted AD-MSCs from a harmful microenvironment in the infarcted myocardium, thereby augmenting cardiac repair and function in future regenerative medicine strategies.

Materials and Methods

Animals

Fluc⁺-eGFP⁺ transgenic mice (Tg [*Fluc-egfp*]) were bred in a C57BL/6a background to constitutively express firefly luciferase (Fluc) and eGFP in all tissue and organs. C57BL/6a mice (Tg [*Fluc-egfp*] inbred strain, Fluc-eGFP⁻, $n = 100$, male, 8 weeks old, 20–25 g) were used for the MI model. All

animal procedures were conducted in conformity with the National Institutes of Health Guide for the Care and Use of Laboratory Animals, and all experiments were performed in accordance with the Helsinki declaration.

Isolation and culture of AD-MSCs

AD-MSCs were isolated from Fluc⁺-eGFP⁺ transgenic mice as previously described (7). In brief, adipose tissue was harvested from β -Actin-Fluc-GFP transgenic mice. Then, the tissue was washed with phosphate-buffered saline (PBS) and mechanically chopped before digestion with 0.2% collagenase I (Sigma) for 1 h at 37°C with intermittent shaking. The digested tissue was washed with Dulbecco's modified Eagle's medium (DMEM) (Sigma) containing 15% fetal bovine serum (FBS), and then centrifuged at 1000 rpm for 10 min to remove mature adipocytes. The cell pellet was resuspended in DMEM supplemented with 15% FBS, 100 U/ml penicillin, and 100 μ g/ml streptomycin in a 37°C incubator with 5% CO₂. AD-MSCs reaching 80%–90% confluency were detached with 0.02% ethylenediaminetetraacetic acid (EDTA)/0.25% trypsin (Sigma-Aldrich) for 5 min at room temperature and then replated. Cells between the third and fifth passage were used for experiments.

MI mice model

Male mice weighing 20–25 g were randomly allocated into the following groups with $n=20$ each: (i) Sham group (Sham), (ii) MI+PBS group (MI), (iii) MI+LXR agonist T0901317 group (LXR), (iv) MI+AD-MSCs group (AD-MSCs), (v) MI+AD-MSCs+LXR agonist T0901317 pretreatment before transplantation group (AD-MSCs+LXR Pre), (vi) MI+AD-MSCs transfected with Nrf-2 siRNA+LXR agonist T0901317 (AD-MSCs with Nrf-2 siRNA+LXR), and (vii) MI+AD-MSCs+LXR agonist T0901317 group (AD-MSCs+LXR).

Murine MI was induced by ligation of the left anterior descending (LAD) artery (8). In brief, mice were anesthetized with persistent inhaled 2% isoflurane during the operation. A left thoracotomy was performed, and the pericardium was opened. The LAD was permanently ligated with a 6-0 suture at the level of the left atrium. The ligation was deemed successful when the anterior wall of the left ventricle turned pale. Then, echocardiography was utilized to further confirm that the MI model in mice was successfully constructed. For sham-operated mice, open thoracotomy was performed without suturing of the LAD. AD-MSCs transplantation was performed immediately after MI performance. 1×10^6 AD-MSCs were injected intramyocardially into the peri-infarct areas at two different sites with a total volume of 20 μ l in each animal. Control animals instead received a 20 μ l PBS injection.

The chest cavity was closed in layers with a 4-0 suture. In the LXR group, T0901317 (Cayman Chemical Company) was administered (20 mg/kg/day) by gavage for successive 28 days post-AD-MSCs transplantation.

In vivo monitoring of transplanted mAD-MSCs^{Fluc⁺-eGFP⁺} via bioluminescence imaging

Bioluminescence signal of engrafted mAD-MSCs^{Fluc⁺-eGFP⁺} was detected using an IVIS Kinetic system (Caliper) as previously described. Ten minutes after an intraperitoneal injection of

the reporter probe D-luciferin (150 mg/kg; Caliper), animals were imaged for 5 min on POD 2, 7, 14, 21, and 28 respectively. Bioluminescent signals were analyzed using Living Image[®] 3.1 software (Caliper) and quantified in units of photons/s/cm²/sr.

Analysis of mAD-MSCs^{Fluc⁺-eGFP⁺} engraftment

To further validate the results of *in vivo* BLI for mAD-MSCs^{Fluc⁺-eGFP⁺} survival, five mice were sacrificed and hearts were harvested to find GFP-positive cells at POD 14. The hearts were harvested and cut along the short axis with five pieces from the base to the apex. Serial sections were prepared at 5 μ m thickness. 4',6-diamidino-2-phenylindole (DAPI) was used for nuclear staining (1:1000; Bioworld). Cell engraftment was confirmed by identification of GFP expression under a confocal laser scanning microscope (Olympus FV10i).

Left ventricular functional analysis with echocardiogram

Echocardiography studies were performed with Vevo[®] 2100 ultrasound system (VisualSonics) using a 30-MHz linear array ultrasound transducer on baseline (day-7) and POD 2, 14, and 28 by two blinded investigators. The mice were anesthetized with inhaled 2% isoflurane and placed in a supine position. Both two-dimensional and M-mode images were recorded. The left ventricular end-systolic volume and left ventricular end-diastolic volume were measured to calculate LVEF and FS.

Measurement of infarct size

Mice were euthanized, and hearts were harvested for histological staining at POD 28. A separate set of paraffin-embedded tissue sections were stained using Masson's trichrome, resulting in fibrotic (collagen-enriched) areas that appeared blue while cellular elements appeared red. For 10 randomly selected microscopic fields ($\times 200$ magnification) of each left ventricle, Masson's trichrome-stained myocardial sections were imaged, and the collagen area was calculated as a percentage of the total left ventricular myocardial area. This served as an estimate of infarct size. Measurement was performed by an observer who was blinded to the group assignment *via* Imaging Pro Plus software.

Evaluation of myocardial angiogenesis with immunohistochemical staining

To detect myocardial angiogenesis after MI, CD31 immunohistochemical staining was performed. Tissue sections were blocked with 2% normal goat serum for 30 min and then incubated with polyclonal rabbit antibodies: anti-CD31 (1:100; Bioworld) overnight at 4°C. The process of immunohistochemical staining was performed as previously described. Five sections from the heart of each animal were randomly selected, and images were photographed under $\times 200$ magnification in five vision fields/section. The immunoreactive areas for CD31 were analyzed with Image J software.

Determination of myocardial apoptosis

The cell apoptosis rate in the myocardium was determined on POD 3 by TUNEL staining according to the manufacturer's instructions (In Situ Cell Death Detection Kit; Roche

Applied Science). Cells stained with cardiac troponin I were recognized as the myocardium, and the nucleus stained green was defined as TUNEL positive. DAPI were used to stain all cell nuclei. Six micrographs were randomly selected, and the numbers of healthy or apoptotic cardiomyocytes were counted. The percentage of cardiomyocytes apoptosis was calculated as the percentage of the total numbers of cells that were cardiac troponin I and TUNEL double immunostained positive. All of these assays were performed in a blinded manner.

The siRNA targeting of NF- κ B-p65, Nrf-2, and gp91phox siRNA transfection

Nrf-2 siRNA, NF- κ B-p65 siRNA, gp91phox siRNA, and control siRNA were purchased commercially from GeneChemistry. The sequence of the mouse Nrf-2 siRNA (5'-3') was as follows (RNA): 5'-UCC CGU UUG UAG AUG ACA-3'; 5'-UUGUCAUCUACAAACGGGA-3' (Nrf-2, NCBI Reference Sequence: NM_010902.3). NF- κ B-p65 siRNA: 5'-GUU UCA GCA GCU CCU GAA CTT-3'; 5'-GUU CAG GAG CUG CUG AAA CTG-3' (NF- κ B-p65, NCBI Reference Sequence: NM_009045.4). gp91phox siRNA: 5'-CGUUUCCUCUU UGCUUGG-3'; 5'-CCAGACAAAGAGGAAGACG-3' (gp91phox, NCBI Reference Sequence: NM_007807.5). Control siRNA: 5'-TTC AAG UCC UCG ACG ACU UUG-3'; 5'-CTC AAA GUC GUC CAG CAG UUG-3'. AD-MSCs were seeded onto 60-mm dishes at 24 h before transfection and then transiently transfected with 100 nM Nrf-2 siRNA, NF- κ B-p65 siRNA, or control siRNA per dish at 90% confluence using the lipofectamine 2000 (Invitrogen Life Technology) according to the manufacturer's protocol. Successful knockdown of the target proteins was confirmed by Western blot analysis.

Measurement of myocardial, intracellular, and mitochondrial ROS generation, respectively

ROS generation in myocardium was detected using the ROS fluorescent probe-DHE as previously described. In brief, the isolated hearts were cryostat sectioned (10 μ m) and incubated with DHE probe (2 μ M) in PBS solution for 20 min at 37°C on POD 3. The images were obtained with a fluorescence microscope (Nikon) at 488 nm excitation and 590 nm emission.

Production of intracellular and mitochondrial ROS was assessed by measuring the fluorescence intensity of DCF (2,7-dichlorofluorescein-diacetate [DCFH-DA]; Invitrogen) as previously described. At 1 h after the different treatments, isolated mitochondria and cells were isolated or harvested, washed and re-suspended in PBS, respectively, and then incubated with 2 μ g/ml RHO 123 and 10 μ M DCFH-DA at 37°C in an incubator for 20 min with gentle shaking. The mitochondrial and intracellular fluorescence of DCF was determined in GloMax™ 20/20 Luminometer (Promega).

H/SD injury in vitro

AD-MSCs were stimulated with H/SD injury as previously described (41). Briefly, AD-MSCs were plated in 24-well plates (5 \times 10⁴ cells per well). Twenty-four hours later, AD-MSCs were administrated with PBS, cultured in Hanks buffer. Then, different doses of LXR agonist (1, 5, 10, and 15 μ M) and dimethyl sulfoxide were added into their re-

spective wells for another 24 h. Then, AD-MSCs were exposed to hypoxia (94% N₂-5% CO₂-1% O₂) in an anaerobic system (Thermo Forma) at 37°C for 6 h. After 6 h of either hypoxia or normal conditions, mediums were removed from wells and collected for later ELISA. In the control group, AD-MSCs were maintained at normoxia (95% air-5% CO₂) for equivalent periods.

BLI of mAD-MSCs^{Fluc+ -eGFP+} in vitro

To assess for protective effects of the LXR agonist on AD-MSCs, we assessed cell survival with BLI using the IVIS Kinetic system (Caliper). Briefly, mAD-MSCs^{Fluc+ -eGFP+} in plates after H/SD injury were imaged after D-luciferin was added to each well. Bioluminescent signals were analyzed using Living Image 3.1 software (Caliper) and quantified as average radiance in photons/s/cm²/sr.

ELISA for soluble inflammatory cytokines and growth factors

To examine the amount of IL-6, TNF- α , VEGF, and bFGF in the supernatant of AD-MSCs, measurements were carried out using commercially available ELISA kits (Sen-Xiong Company). In accordance with the manufacturer's instructions, all supernatant was stored at -80°C before measurement and both standards and samples were run in triplicate. OD₄₅₀ was calculated by subtracting the background, and standard curves were plotted.

Quantitative real-time polymerase chain reaction

To investigate basal mRNA expression of LXRs in AD-MSCs, total RNA of cells was isolated using RNeasy (Qiagen) according to the manufacturer's instructions. To generate cDNA, 1 μ g of total RNA was used with the oligo dT primer following the protocol for the First-Strand cDNA Synthesis kit (Amersham Bioscience). Real-time quantitative PCR was performed using an ABI Prism 7900 system (Applied Biosystems). The levels of LXR α and LXR β mRNA expression were normalized to GAPDH mRNA expression level. The sequences of forward primer (FP) and reverse primer (RP) were as follows: LXR α FP: 5'-CGACAGAG CTTCGTCCACAA-3', RP: 5'-GCTCGTTCCCCAGCAT TTT-3'; LXR β FP: 5'-CGTGCCTGGGAATGGTTCT-3', RP: 5'-AGTCTCCTGCCCTCTTCCTT-3'. GAPDH FP: 5'-GCCAAAAGGGTTCATCAT CTC-3', RP: 5'-GTAGAG GC AGGGATGATGTTTC-3'.

Western blot assay

AD-MSCs in the plate after H/SD treatment were washed twice with cold PBS, then lysed with RIPA buffer (1% Triton X-100, 20 mM of Tris [PH=7.5]), 10 mM of EDTA, 0.02% sodium azide, and protease-inhibitors such as leupeptin for about 1 h. Cell lysates were centrifuged at 10,000 g at 4°C for 20 min. Lysates were boiled in sample buffer for 5 min. The proteins were then subjected to 10% SDS-PAGE and transferred to nitrocellulose membranes using a semi-dry electroblotting system. After blocking with 5% skim milk in PBS, the membranes were incubated with diluted polyclonal rabbit anti-mouse LXR α (1:1000; Abcam), LXR β (1:1000; Abcam), NADPH oxidase anti-NOX2/gp91^{phox} (1:500; Bioss), NF- κ B-p65 (1:1000), MyD88 (1:1000), TRAF-6 (1:1000),

TLR4 (1:1000), I κ B α (1:1000), p-I κ B α (1:1000), Keap-1 (1:1000), Nrf-2 (1:1000), HO-1 (1:1000; all from Bioworld), and a monoclonal anti- β -actin antibody (1:1000; Abcam) at 4°C overnight. After washing and further incubation with appropriate secondary antibodies conjugated with horseradish peroxidase (dilution: 1:5000 in TBST) at 37°C for 60 min, bands were visualized using an enhanced chemiluminescence system (ECL; Amersham). Densitometric analysis of Western blots was carried out using VisionWorks LS, version 6.7.1.

Statistical analysis

The results are expressed as mean \pm SEM. Statistical differences between different groups were evaluated with Prism 5.0 (GraphPad Software, Inc.). Groups were compared using Student's two-tailed unpaired *t* test or a one-way ANOVA analysis, followed by Dunnett's *post hoc* test as appropriate. Statistical significance was set at *p* < 0.05.

Acknowledgments

This work was supported by the National Funds for Distinguished Young Scientists of China (81325009), the National Nature Science Foundation of China (No. 81270168, No. 81090274, No. 81227901) (FCao BWS12J037), Innovation Team Development Grant by China Department of Education (IRT1053), the National Basic Research Program of China (2012CB518101), and Shanxi Province Program (2013K12-02-03).

Author Disclosure Statement

The authors declare that no competing financial interests exist.

References

- Bianco P, Cao X, Frenette PS, Mao JJ, Robey PG, Simmons PJ, and Wang CY. The meaning, the sense and the significance: translating the science of mesenchymal stem cells into medicine. *Nat Med* 19: 35–42, 2013.
- Cao F, van der Bogt KE, Sadrzadeh A, Xie X, Sheikh AY, Wang H, Connolly AJ, Robbins RC, and Wu JC. Spatial and temporal kinetics of teratoma formation from murine embryonic stem cell transplantation. *Stem Cells Dev* 16: 883–891, 2007.
- Cheng TH, Cheng PY, Shih NL, Chen IB, Wang DL, and Chen JJ. Involvement of reactive oxygen species in angiotensin II-induced endothelin-1 gene expression in rat cardiac fibroblasts. *J Am Coll Cardiol* 42: 1845–1854, 2003.
- Cui G, Shan L, Hung M, Lei S, Choi I, Zhang Z, Yu P, Hoi P, Wang Y, and Lee SM. A novel Danshensu derivative confers cardioprotection via PI3K/Akt and Nrf2 pathways. *Int J Cardiol* 168: 1349–1359, 2013.
- Dai DF, Johnson SC, Villarín JJ, Chin MT, Nieves-Cintrón M, Chen T, Marcinek DJ, Dorn GW, 2nd, Kang YJ, Prolla TA, Santana LF, and Rabinovitch PS. Mitochondrial oxidative stress mediates angiotensin II-induced cardiac hypertrophy and Galphaq overexpression-induced heart failure. *Circ Res* 108: 837–846, 2011.
- Dikalov SI, Nazarewicz RR, Bikineyeva A, Hilenski L, Lassègue B, Griendling KK, Harrison DG, and Dikalova AE. Nox2-induced production of mitochondrial superoxide in angiotensin II-mediated endothelial oxidative stress and hypertension. *Antioxid Redox Signal* 20: 281–294, 2014.
- Fan W, Cheng K, Qin X, Narsinh KH, Wang S, Hu S, Wang Y, Chen Y, Wu JC, Xiong L, and Cao F. mTORC1 and mTORC2 play different roles in the functional survival of transplanted adipose-derived stromal cells in hind limb ischemic mice via regulating inflammation *in vivo*. *Stem Cells* 31: 203–214, 2013.
- Fan W, Li C, Qin X, Wang S, Da H, Cheng K, Zhou R, Tong C, Li X, Bu Q, Li C, Han Y, Ren J, and Cao F. Adipose stromal cell and sarpogrelate orchestrate the recovery of inflammation-induced angiogenesis in aged hindlimb ischemic mice. *Aging Cell* 12: 32–41, 2013.
- Gao E, Lei YH, Shang X, Huang ZM, Zuo L, Boucher M, Fan Q, Chuprun JK, Ma XL, and Koch WJ. A novel and efficient model of coronary artery ligation and myocardial infarction in the mouse. *Circ Res* 107: 1445–1453, 2010.
- Gordon JW, Shaw JA, and Kirshenbaum LA. Multiple facets of NF- κ B in the heart: to be or not to NF- κ B. *Circ Res* 108: 1122–1132, 2011.
- Hannedouche S, Zhang J, Yi T, Shen W, Nguyen D, Pereira JP, Guerini D, Baumgarten BU, Roggo S, Wen B, Knochenmuss R, Noel S, Gessier F, Kelly LM, Vanek M, Laurent S, Preuss I, Miault C, Christen I, Karuna R, Li W, Koo DI, Suply T, Schmedt C, Peters EC, Falchetto R, Katopodis A, Spanka C, Roy MO, Dethoux M, Chen YA, Schultz PG, Cho CY, Seuwen K, Cyster JG, and Sailer AW. Oxysterols direct immune cell migration via EB12. *Nature* 475: 524–527, 2011.
- Herrmann JL, Abarbanell AM, Weil BR, Manukyan MC, Poynter JA, Brewster BJ, Wang Y, and Meldrum DR. Optimizing stem cell function for the treatment of ischemic heart disease. *J Surg Res* 166: 138–145, 2011.
- Hochmuth CE, Biteau B, Bohmann D, and Jasper H. Redox regulation by Keap1 and Nrf2 controls intestinal stem cell proliferation in *Drosophila*. *Cell Stem Cell* 8: 188–199, 2011.
- Hsiao LC, Carr C, Chang KC, Lin SZ, and Clarke K. Stem cell-based therapy for ischemic heart disease. *Cell Transplant* 22: 663–675, 2013.
- Hyun JS, Tran MC, Wong VW, Chung MT, Lo DD, Montoro DT, Wan DC, and Longaker MT. Enhancing stem cell survival *in vivo* for tissue repair. *Biotechnol Adv* 31: 736–743, 2013.
- Janowski BA, Willy PJ, Devi TR, Falck JR, and Mangelsdorf DJ. An oxysterol signalling pathway mediated by the nuclear receptor LXR alpha. *Nature* 383: 728–731, 1996.
- Joseph SB, Bradley MN, Castrillo A, Bruhn KW, Mak PA, Pei L, Hogenesch J, O'Connell RM, Cheng G, Saez E, Miller JF, and Tontonoz P. LXR-dependent gene expression is important for macrophage survival and the innate immune response. *Cell* 119: 299–309, 2004.
- Joseph SB, Castrillo A, Laffitte BA, Mangelsdorf DJ, and Tontonoz P. Reciprocal regulation of inflammation and lipid metabolism by liver X receptors. *Nat Med* 9: 213–219, 2003.
- Kim BS, Jung JS, Jang JH, Kang KS, and Kang SK. Nuclear argonaute 2 regulates adipose tissue-derived stem cell survival through direct control of miR10b and selenoprotein N1 expression. *Aging Cell* 10: 277–291, 2011.
- Lei P, Baysa A, Nebb HL, Valen G, Skomedal T, Osnes JB, Yang Z, and Haugen F. Activation of Liver X receptors in the heart leads to accumulation of intracellular lipids and attenuation of ischemia-reperfusion injury. *Basic Res Cardiol* 108: 323, 2013.
- Li H, Zuo S, He Z, Yang Y, Pasha Z, Wang Y, and Xu M. Paracrine factors released by GATA-4 overexpressed mesenchymal stem cells increase angiogenesis and cell survival. *Am J Physiol Heart Circ Physiol* 299: H1772–H1781, 2010.

21. Li S, Tao L, Jiao X, Liu H, Cao Y, Lopez B, Luan RH, Christopher T, and Ma XL. TNF α -initiated oxidative/nitrative stress mediates cardiomyocyte apoptosis in traumatic animals. *Apoptosis* 12: 1795–1802, 2007.
22. Mohammadzadeh M, Halabian R, Gharehbaghian A, Amirzadeh N, Jahanian-Najafabadi A, Roushandeh AM, and Roudkenar MH. Nrf-2 overexpression in mesenchymal stem cells reduces oxidative stress-induced apoptosis and cytotoxicity. *Cell Stress Chaperones* 17: 553–565, 2012.
23. Morales JR, Ballesteros I, Deniz JM, Hurtado O, Vivancos J, Nombela F, Lizasoain I, Castrillo A, and Moro MA. Activation of liver X receptors promotes neuroprotection and reduces brain inflammation in experimental stroke. *Circulation* 118: 1450–1459, 2008.
24. Ohtsu H, Frank GD, Utsunomiya H, and Eguchi S. Redox-dependent protein kinase regulation by angiotensin II: mechanistic insights and its pathophysiology. *Antioxid Redox Signal* 7: 1315–1326, 2005.
25. Qu Z, Xu H, Tian Y, and Jiang X. Atorvastatin improves microenvironment to enhance the beneficial effects of BMSCs therapy in a rabbit model of acute myocardial infarction. *Cell Physiol Biochem* 32: 380–389, 2013.
26. Rehman J, Traktuev D, Li J, Merfeld-Clauss S, Temm-Grove CJ, Bovenkerk JE, Pell CL, Johnstone BH, Conside RV, and March KL. Secretion of angiogenic and antiapoptotic factors by human adipose stromal cells. *Circulation* 109: 1292–1298, 2004.
27. Sacchetti P, Sousa KM, Hall AC, Liste I, Steffensen KR, Theofilopoulos S, Parish CL, Hazenberg C, Richter LA, Hovatta O, Gustafsson JA, and Arenas E. Liver X receptors and oxysterols promote ventral midbrain neurogenesis *in vivo* and in human embryonic stem cells. *Cell Stem Cell* 5: 409–419, 2009.
28. Segers VF and Lee RT. Stem-cell therapy for cardiac disease. *Nature* 451: 937–942, 2008.
29. Steffensen KR, Jakobsson T, and Gustafsson JA. Targeting liver X receptors in inflammation. *Expert Opin Ther Targets* 17: 977–990, 2013.
30. Tan J, Weil BR, Abarbanell AM, Wang Y, Herrmann JL, Dake ML, and Meldrum DR. Ablation of TNF- α receptors influences mesenchymal stem cell-mediated cardiac protection against ischemia. *Shock* 34: 236–242, 2010.
31. Tang YL, Tang Y, Zhang YC, Qian K, Shen L, and Phillips MI. Improved graft mesenchymal stem cell survival in ischemic heart with a hypoxia-regulated heme oxygenase-1 vector. *J Am Coll Cardiol* 46: 1339–1350, 2005.
32. Theofilopoulos S, Wang Y, Kitambi SS, Sacchetti P, Sousa KM, Bodin K, Kirk J, Salto C, Gustafsson M, Toledo EM, Karu K, Gustafsson JA, Steffensen KR, Ernfors P, Sjövall J, Griffiths WJ, and Arenas E. Brain endogenous liver X receptor ligands selectively promote midbrain neurogenesis. *Nat Chem Biol* 9: 126–133, 2013.
33. Urao N and Ushio-Fukai M. Redox regulation of stem/progenitor cells and bone marrow niche. *Free Radic Biol Med* 54: 26–39, 2013.
34. Wang FW, Wang Z, Zhang YM, Du ZX, Zhang XL, Liu Q, Guo YJ, Li XG, and Hao AJ. Protective effect of melatonin on bone marrow mesenchymal stem cells against hydrogen peroxide-induced apoptosis *in vitro*. *J Cell Biochem* 114: 2346–2355, 2013.
35. Wang L, Li YL, Zhang CC, Cui W, Wang X, Xia Y, Du J, and Li HH. Inhibition of toll-like receptor 2 reduces cardiac fibrosis by attenuating macrophage-mediated inflammation. *Cardiovasc Res* 101: 383–392, 2014.
36. Wang WE, Yang D, Li L, Wang W, Peng Y, Chen C, Chen P, Xia X, Wang H, Jiang J, Liao Q, Li Y, Xie G, Huang H, Guo Y, Ye L, Duan DD, Chen X, Houser SR, and Zeng C. Prolyl hydroxylase domain protein 2 silencing enhances the survival and paracrine function of transplanted adipose-derived stem cells in infarcted myocardium. *Circ Res* 113: 288–300, 2013.
37. Wang X, Zhao T, Huang W, Wang T, Qian J, Xu M, Kranias EG, Wang Y, and Fan GC. Hsp20-engineered mesenchymal stem cells are resistant to oxidative stress via enhanced activation of Akt and increased secretion of growth factors. *Stem Cells* 27: 3021–3031, 2009.
38. Wei H, Li Z, Hu S, Chen X, and Cong X. Apoptosis of mesenchymal stem cells induced by hydrogen peroxide concerns both endoplasmic reticulum stress and mitochondrial death pathway through regulation of caspases, p38 and JNK. *J Cell Biochem* 111: 967–978, 2010.
39. Wu J, Li J, Zhang N, and Zhang C. Stem cell-based therapies in ischemic heart diseases: a focus on aspects of microcirculation and inflammation. *Basic Res Cardiol* 106: 317–324, 2011.
40. Wu JY, Chen CH, Wang CZ, Ho ML, Yeh ML, and Wang YH. Low-power laser irradiation suppresses inflammatory response of human adipose-derived stem cells by modulating intracellular cyclic AMP level and NF- κ B activity. *PLoS One* 8: e54067, 2013.
41. Zhang Z, Li S, Cui M, Gao X, Sun D, Qin X, Narsinh K, Li C, Jia H, Li C, Han Y, Wang H, and Cao F. Rosuvastatin enhances the therapeutic efficacy of adipose-derived mesenchymal stem cells for myocardial infarction via PI3K/Akt and MEK/ERK pathways. *Basic Res Cardiol* 108: 333, 2013.
42. This reference has been deleted.

Address correspondence to:
 Dr. Feng Cao
 Department of Cardiology
 PLA General Hospital
 Beijing 100853
 China

E-mail: wind8828@gmail.com

Date of first submission to ARS Central, October 12, 2013; date of final revised submission, May 29, 2014; date of acceptance, June 7, 2014.

Abbreviations Used

AD-MSCs = adipose-derived mesenchymal stem cells
 AI = apoptotic index
 bFGF = basic fibroblast growth factor
 BLI = bioluminescence imaging
 DAPI = 4',6-diamidino-2-phenylindole
 DCF = dichlorofluorescein
 DCFH-DA = 2,7-dichlorofluorescein-diacetate
 DHE = dihydroethidium
 DMEM = Dulbecco's modified Eagle's medium
 DMSO = dimethyl sulfoxide
 EDTA = ethylenediaminetetraacetic acid
 eGFP = enhanced green fluorescence protein
 FBS = fetal bovine serum
 FP = forward primer
 FS = fraction shortening
 H/SD = hypoxia/serum deprivation

Abbreviations Used (Cont.)

IL-6 = interleukin-6
LAD = left anterior descending
LVEF = left ventricular ejection fraction
LXR = liver X receptor
MI = myocardial infarction
PBS = phosphate-buffered saline
PCR = polymerase chain reaction

PI = propidium iodide
POD = postoperative days
ROS = reactive oxygen species
RP = reverse primer
TNF- α = tumor necrosis factor- α
TUNEL = terminal deoxy-nucleotidyl transferase-
mediated dUTP nick end labeling
VEGF = vascular endothelial growth factor